Physical foundations and basic properties of magnetic skyrmions

Alexei N. Bogdanov and Christos Panagopoulos

Abstract | Magnetic skyrmions (or vortices) are spatially inhomogeneous spin textures localized in nanoscale cylindrical regions. Their small size and unique stability make skyrmions attractive for the study of spin topology and technologies wherein information is carried by the electron spin in addition to, or instead of, the electron charge. Despite advances in the synthesis of materials in which axisymmetric magnetic skyrmions can be stabilized and characterized, there has been relatively slow progress in elucidating the basic properties. This Perspective aims to bridge this gap by delivering a brief, accessible guide to the physical principles governing magnetic skyrmions.

Magnetic skyrmions were introduced theoretically in 1989 as a new type of two-dimensional spatially localized state, stabilized in magnetic materials with broken inversion symmetry[1]. Typically, they emerge as right circular cylinders of axisymmetric spin texture (FIG. 1a) at magnetic fields, **H**, above saturation[1–4]. In Bloch-type magnetic skyrmions (FIG. 1b), for example, the magnetization vector **M** rotates with a fixed rotation sense in the plane perpendicular to the propagation vector **p**, namely, from an antiparallel direction at the axis to a parallel direction at distances far from the centre (FIG. 1c). Bloch-type skyrmions stabilize in ferromagnets with D_n symmetry[1,4] and in the extended group of cubic helimagnets[3,5–8]. This is just one of the five possible skyrmion core configurations in non-centrosymmetric uniaxial ferromagnets (BOX 1)[1,4].

The study of magnetic skyrmions emerged from an apparent paradox. Mathematically, two-dimensional and three-dimensional localized structures are unstable in most condensed-matter systems (the Hobart–Derrick theorem)[9]. Accordingly, localized structures such as magnetic skyrmions are not expected to exist. Hence, once induced, they would rapidly collapse into linear singularities. However, magnetic materials with broken inversion symmetry do not obey the 'prohibition' rule imposed by the Hobart–Derrick theorem[1]. In these low-symmetry systems, magnetic interactions imposed by the handedness of the underlying crystallographic structure (known as Dzyaloshinskii–Moriya interactions[10]) provide a physical mechanism that prevents the collapse and stabilizes axisymmetric localized states with finite sizes[1,11]. The experimental search for magnetic skyrmions commenced two decades after the theoretical prediction[5,6], leading to the discovery of skyrmions in several groups of magnetic crystals, as well as in synthetic nanolayers and multilayers of magnetic metals[12–19]. Advances in modern experimental methods and data analysis have enabled the identification of topological spin textures and detailed investigations of their evolution with field and temperature[13–17].

The practical application of skyrmions indicated early on in theoretical studies[11] helped to formulate a new paradigm in magnetic storage technologies. During the past decade, various device concepts based on magnetic skyrmions have emerged, providing the basis for highly mobile, low-power and super-dense magnetic data storage, and other spintronic applications[20,21]. Subsequently, the field has been enriched by numerous experimental observations and results of numerical simulations. Despite impressive experimental accomplishments and encouraging practical prospects, there has been relatively slow progress in understanding the physical principles. Although it is generally acknowledged that the mathematical formalism of magnetic skyrmions belongs to the physics of solitons, this domain of nonlinear physics is rather unfamiliar to modern multidisciplinary materials research. As a result, efforts to gain a coherent physical insight from the amount of experimental data remain scarce.

In this Perspective, we initiate a discussion on the fundamental properties of magnetic skyrmions as a special class of 'self-supporting' localized states (solitons) and expound their stabilization mechanism. Using established mathematical tools of nonlinear physics, the properties of magnetic skyrmions can be expressed in the language of soliton physics (BOX 1) and shown to emerge as axisymmetric strings with a fixed direction of rotation. Comparison of physical modelling with state-of-the-art experiments demonstrates the essential features of isolated skyrmions (FIG. 2) and skyrmion lattices (FIG. 3).

Solitary waves and solitons

Magnetic skyrmions (FIG. 1) belong to pattern formation phenomena that are widespread in nature, manifesting as countable objects ('particles') in continuous fields. Such patterns are characterized by spatial and temporal dimensions. Tornados and typhoons, solitary surface ocean waves, and spherulites in chiral liquid crystals are just a few examples.

In most physical systems, particle-like patterns emerge as unstable dynamic excitations, which gradually decay into a homogeneous state (as in tornados and typhoons). However, there exists a special class of self-supporting particle-like objects known as solitons[22–24]. The canonical case of solitons as travelling solitary waves on a water surface is described in BOX 2. Commonly, once formed, such surface waves gradually spread and eventually decay. However, in 1834, John Scott Russell recognized an unusual stability of solitary surface waves travelling through shallow water channels. Following this observation, in 1871 Joseph Boussinesq demonstrated theoretically that solitary waves in shallow water are in fact stabilized by the seabed. These studies were developed further by Diederik Korteweg and Gustav de Vries in 1898, who provided a detailed analysis of the

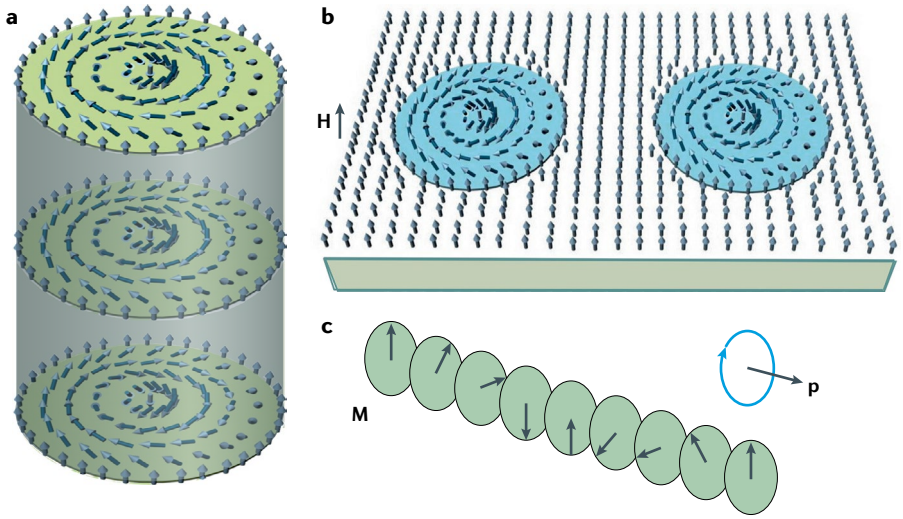

Fig. 1 | **Magnetic skyrmions. a**–**c** | Magnetic skyrmions are axisymmetric nanoscale right cylinders (panel **a**) emerging as ensembles of weakly repulsive 'particles' at an applied magnetic field **H** in homogeneously magnetized ferromagnets (panel **b**). Panels **a**–**c** depict the most common ('Bloch-type') skyrmion configurations with the magnetization **M** rotating in the plane perpendicular to the propagation direction **p** (panel **c**).

localized and periodic solutions for shallow water waves (BOX 2)[22].

The discovery of intrinsically stable, localized states introduced a new physical paradigm: a 'solid' particle-like object can be induced in continuous media and easily controlled and manipulated by external forces. This breakthrough was appreciated only decades later, in the second half of the twentieth century (the term soliton was coined by Martin Kruskal and Norman Zabusky in 1969[25]). At the time, numerical simulations allowed for new solutions of solitonic states and subsequently the development of a new domain in nonlinear science: soliton physics[22,25].

Skyrmion terminology

The solution for a shallow water soliton (see BOX 2) and the underlying physical mechanism stabilizing this state is a prototype for all solitonic states[24], including magnetic skyrmions. Originally, these solitonic states were introduced as 'magnetic vortices'[1], and they were later renamed magnetic skyrmions. The term skyrmion was coined in the early 1980s to designate solutions for three-dimensional solitons, for the field models[23] introduced by Tony Skyrme[26]. Subsequently, it has been applied to multidimensional non-singular localized states with non-trivial topology. In this extended meaning, skyrmion does not describe a fundamental entity with shared physical properties such as electrons, protons or quarks. Instead, it serves as an umbrella term for a variety of textures, heuristically attributed to topologically non-trivial, smooth localized structures in diverse areas of physics, from cosmology to condensed matter[27].

Following this trend, the term skyrmion has been used to designate magnetic localized states with a diverse physical nature, such as magnetic bubble domains stabilized by demagnetization effects[28], solitonic states due to competing exchange interactions (frustration)[29] or Belavin–Polyakov instantons[4,23]. Notably, magnetic skyrmions are not 'topologically protected localized states'. The non-trivial topology protects them from unwinding into saturated states but does not prevent them from collapsing into a linear singularity — a line with antiparallel magnetization — in the saturated phase. The presence of magnetic skyrmions with well-defined sizes is due to the stabilization supported by Dzyaloshinskii–Moriya interactions[1]. Further examples of solitonic states and associated stabilization mechanisms are discussed in the section on 'kinsmen' of magnetic skyrmions.

Isolated magnetic skyrmions

Basic model. Magnetically ordered states (ferromagnetic, antiferromagnetic and so on) are governed by quantum mechanical exchange coupling[30]. However, many magnetically ordered materials can be described by classical field models with respect to the magnetization vector **M** (REF.[28]). Magnetic states in materials with broken spatial inversion symmetry can be described by the basic model[10]

$$w(\mathbf{M}) = A(\partial_i \mathbf{M})^2 + V(\mathbf{M}) + w_{\mathrm{D}}(\mathbf{M}) \qquad (1)$$

where w is the energy density and $A(\partial_i \mathbf{M})^2 \equiv \sum_{i,j=1}^{3} (\partial M_j / \partial x_i)^2$ is the exchange energy with stiffness constant A. $V(\mathbf{M})$ is the 'potential' term, including internal magnetic interactions and interactions with applied magnetic fields. For uniaxial ferromagnets, $V(\mathbf{M}) = K[1 - (\mathbf{M} \cdot \mathbf{n})^2] + \mu_0[MH - \mathbf{M} \cdot \mathbf{H}]$ includes the uniaxial magnetocrystalline anisotropy with coefficient K ($\mathbf{n}$ is the unit vector along the high symmetry axis), and the Zeeman energy; μ_0 is vacuum permeability.

In this model, the Dzyaloshinskii–Moriya energy density, $w_{\mathrm{D}}(\mathbf{M})$ is described by a combination of functionals that are linear in the first spatial derivatives of **M** ('Lifshitz invariants'):

$$\mathcal{L}_{ij}^{(k)} = M_i \partial M_j / \partial x_k - M_j \partial M_i / \partial x_k \qquad (2)$$

Here, the energy contributions $\mathcal{L}_{ij}^{(k)}$ favour modulated states with magnetization rotation in the (i,j)-planes and propagation direction along the k-axis. Importantly, they provide the stabilization mechanism for helical states[10] and magnetic skyrmions[1,2]. For example, in non-centrosymmetric cubic ferromagnets, which belong to the crystallographic class T (for example, MnSi, FeGe, Cu_2OSeO_3), $w_{\mathrm{D}}(\mathbf{M}) = D(\mathcal{L}_{yx}^{(z)} + \mathcal{L}_{xz}^{(y)} + \mathcal{L}_{zy}^{(x)}) = D\boldsymbol{M} \times \mathrm{curl}(\boldsymbol{M})$, where D is the Dzyaloshinskii–Moriya constant (REF.[31]). These three Lifshitz invariants favour a magnetization rotation that lies in the planes perpendicular to the propagation directions (as in Bloch domain walls[28]). However, in uniaxial ferromagnets with C_{nv} symmetry ($n = 2, 3, 6$), $w_{\mathrm{D}}(\mathbf{M}) = D(\mathcal{L}_{xz}^{(x)} - \mathcal{L}_{yz}^{(y)})$. In this case, the magnetization rotates along the propagation directions (as in Néel domain walls[28]).

The energy functional in Eq. 1 includes interactions that are essential to stabilize magnetic skyrmions. However, it neglects other energy contributions, such as demagnetization effects, magnetoelastic coupling, surface/interface-induced interactions and instabilities, as well as edge effects. The solutions derived within this simplified model[1–4,11,32] describe the fundamental properties of skyrmionic states in non-centrosymmetric ferromagnets. They provide the conceptual and mathematical basis for theoretical investigations of complex magnetic phenomena in magnetic nanolayers[33–38] and artificial magnetic multilayers with intrinsic or induced Dzyaloshinskii–Moriya interactions (see, for example, REFS[39,40]).

Axisymmetric magnetic skyrmions. The solutions of Eq. 1 are $\theta(\rho)$, $\psi(\phi)$ for isolated skyrmions (see BOX 1 and FIG. 2a,b). Three types of magnetic skyrmion have so far been identified in non-centrosymmetric ferromagnets. These are type-I (or Bloch-type) skyrmions, which have been observed in bulk samples and nanolayers of non-centrosymmetric cubic helimagnets[7,8,14,19,33,34,41]; type-II (or Néel-type) skyrmions, discovered in rhombohedral ferromagnets GaV_4S_8 and GaV_4Se_8 with C_{3v} symmetry (these belong to a group of lacunar spinels)[15], as well as in FePt/Ir nanolayers (see FIG. 2c) with surface-induced Dzyaloshinskii–Moriya interactions[4,13,35]; and type-III skyrmions, observed in non-centrosymmetric Heusler alloys with D_{2d} symmetry[19]. Solutions $\theta(\rho)$ (as in FIG. 2a) are derived from Eq. 8 in BOX 1 and are described by the three characteristic parameters shown in Eq. 10[4,36].

A typical solution for the magnetization profiles $\theta(\rho)$ is shown in FIG. 2b, together with experimental data for magnetic skyrmions in FePt/Ir nanolayers[4]. The skyrmion diameter L_s decreases with increasing applied magnetic field (FIG. 2b)[11,36]. In contrast to magnetic bubble domains, which collapse in moderate fields[28], skyrmions persist even in high fields[11]. However, they lose radial stability and collapse when the applied magnetic field compresses them to sizes of just a few lattice constants[4,37].

Two scenarios of skyrmion evolution. In the presence of a high magnetic field, the energy of magnetic skyrmions E (Eq. 3) is positive. In this case, skyrmions exist as locally stable two-dimensional particles (cylinders) in a homogeneously saturated matrix (FIGS 1a and 2). At lower fields, however, the skyrmion energy is negative. Thus, for $E<0$, a spatially modulated phase composed of skyrmion 'cells' (for instance, in the form of a hexagonal lattice as in FIG. 3a) would have lower energy than in the saturated state. $E(H,K)=0$, with H the magnetic field and K the anisotropy parameter, yields the critical field of the phase transition between the saturated state and a skyrmion lattice, $H_s(K)$ (REFS[2,4]). In particular, for cubic helimagnets, $H_s(0)=0.801H_D$, with H_D being the saturation magnetic field (FIG. 2b)[2]. Notably, the emergence of skyrmion lattices within the saturated phase, that is, below $H_s(K)$, is possible if isolated skyrmions can be easily nucleated. Otherwise, the saturated phase (with embedded isolated skyrmions) would persist as a metastable state, even below H_s. As a matter of fact, the presence of isolated magnetic skyrmions is constrained by the elliptical instability field, $H_{el}(K)$ (REF.[11]). In this case, isolated skyrmions strip out abruptly into bands with one-dimensional helical modulations, and in the case of

Box 1 | **Solutions for magnetic skyrmions**

For the theoretical analysis of magnetic skyrmions, it is helpful to use spherical coordinates for the magnetization vector **M** and cylindrical coordinates for the spatial variables **r**:

$$\mathbf{M}(\mathbf{r}) = M(\sin\theta\cos\psi,\ \sin\theta\sin\psi,\ \cos\theta),\ \mathbf{r} = (\rho\cos\phi, \rho\sin\phi,\ z). \quad (7)$$

Within the simplified model in Eq. 1, the solutions for magnetic skyrmions are reduced to the form $\theta(\rho)$,$\psi(\phi)$ (that is, axisymmetric and homogeneous along the skyrmion axis, z)[1]. For non-centrosymmetric classes of uniaxial ferromagnets, solutions $\psi=\psi(\phi)$ have been derived in analytical form[1].

In panels **a**–**e**, the in-plane projections of the magnetization vector describe five different skyrmion core configurations[1–4] (here D_n, C_{nv}, C_n, S_4 and D_{2d} are the standard notations for crystal symmetries). Note that in ferromagnets with C_n and S_4 symmetries, γ is a constant phase angle determined by the ratio of the competing Dzyaloshinskii–Moriya interactions along orthogonal axes. For the five types of skyrmions, the equilibrium profiles $\theta(\rho)$ are derived from equation

$$A\left(\frac{d^2\theta}{d^2\rho}+\frac{1}{\rho}\frac{d\theta}{d\rho}-\frac{1}{\rho^2}\sin\theta\cos\theta\right)-\frac{D}{\rho}\sin^2\theta+f(\theta)=0, \quad (8)$$

with boundary conditions $\theta(0)=\pi$ and $\theta(\infty)=0$. Here, A is the exchange stiffness constant, D is the Dzyaloshinskii–Moriya constant, and $f(\theta)=-K\sin\theta\cos\theta-\mu_0MH\sin\theta$, with K the anisotropy parameter, is a 'potential' term, including magnetic interactions that are independent of spatial gradients. The reduced energy

$$E=(2\pi)^{-1}\int_0^{2\pi}d\phi\int_0^{\infty}w(\theta,\psi)\rho d\rho, \quad (9)$$

where w is the energy functional in Eq. 1, gives the difference between the magnetic skyrmion energy and the energy of the saturated state ($\theta=0$). The coordinate system in Eq. 7 introduces three characteristic parameters:

$$L_D=4\pi A/|D|,\quad \mu_0H_D=D^2M/(2A),\quad K_0=D^2/(4A), \quad (10)$$

where L_D is the period of helical modulations at zero field and anisotropy, H_D is the saturation magnetic field and K_0 the critical value of uniaxial anisotropy (see FIG. 2b,c).

Panels **f** and **g** depict solutions of the initial value problem $\theta(0)=\pi$, $d\theta/d\rho(0)=-\eta$ for Eq. 8 with $H=0$, $K=2.8K_0$. Profiles $\theta_{(\eta)}(\rho)$ (panel **f**) and the corresponding phase portraits ($\theta_{(\eta)}$,$d\theta_{(\eta)}/d\rho$) (panel **g**) are shown for different values of η. In phase space ($\theta_{(\eta)}$,$d\theta_{(\eta)}/d\rho$) (panel **f**), localized solutions correspond to separatrix solutions (trajectory B in panel **f**). We note that localized solutions exist only for non-zero values of D. In centrosymmetric ferromagnets where $D=0$, all phase trajectories end in one of the poles (for details, see REFS[4,32]).

All panels adapted from REF.[4], CC BY 3.0.

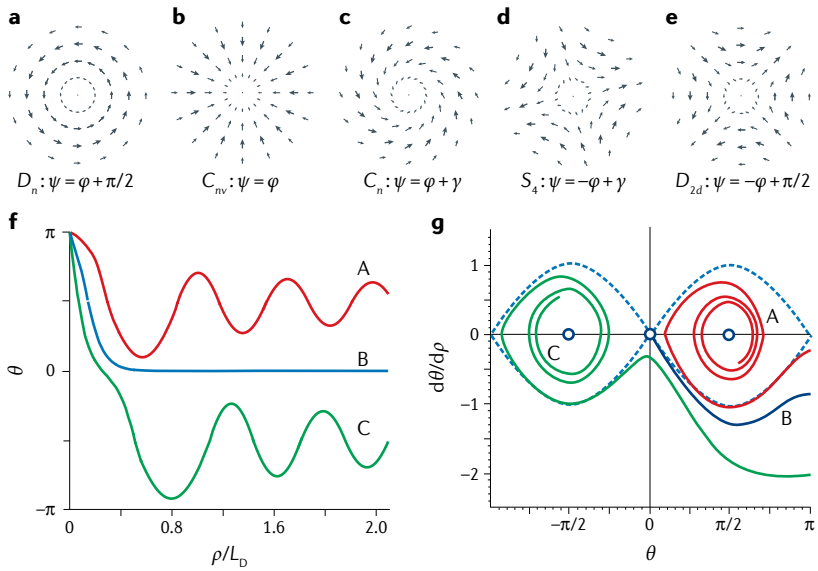

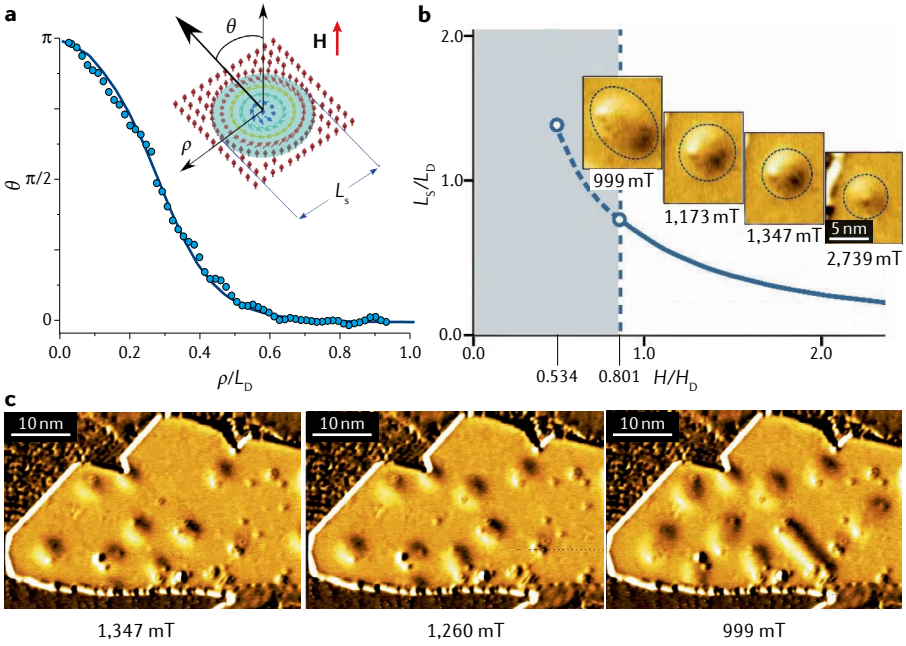

Fig. 2 | **Isolated skyrmions in the saturated state. a** | Magnetization profile in θ and (ρ/L_D) coordinates, where θ and ρ are spherical and cylindrical coordinates as in BOX 1, and L_D is the period of helical modulations at zero field and anisotropy, for an isolated skyrmion at high magnetic fields **H** (filled circles are data from spin-polarized scanning tunnelling microscopy in a FePt/Ir (111) thin film[4]). The solid line is a fit to the data of the solution to Eq. 1 for anisotropy parameters ratio $K/K_0 = 1.3$, magnetic field ratio $H/H_D = 0.32$, with H_D the saturation magnetic field and K_0 the critical value of uniaxial anisotropy; $\mu_0 H = 1.11$ T and $L_D = 6.44$ nm. The inset illustrates the definition of θ, ρ and L_s, the isolated skyrmion size. **b** | Equilibrium values of L_s as a function of applied magnetic field for zero uniaxial anisotropy[2]. The insets show spin-polarized scanning tunnelling microscopy images of an isolated skyrmion at different values of the applied magnetic field (adapted from REF.[4]). The dashed vertical line shows the transition from a skyrmion lattice (grey area) to a saturated state. **c** | Spin-polarized scanning tunnelling microscopy images of magnetic skyrmions in a FePt/Ir (111) thin film for different values of applied magnetic field[4]. The values of $\mu_0 H$ are shown under each sub-panel. Panels **a**, **b** and **c** adapted from REF.[4], CC BY 3.0.

zero anisotropy we have $H_{el}(0) = 0.534 H_D$ (FIG. 2c).

Therefore, isolated skyrmions that emerge as ensembles of weakly repulsive particles in the saturated phase offer two scenarios of evolution with decreasing magnetic field. Either they condense into spatially modulated phases (that is, into skyrmion lattices) below H_s, or they remain as localized states in the metastable saturated phase and strip out into one-dimensional helical states at H_{el}. Indeed, spontaneous nucleation of skyrmion lattices on decreasing the applied magnetic field was observed in wedged nanolayers of cubic helimagnets where magnetic skyrmions were nucleated at the edges and moved to the centre of the sample[38,42].

Spin-polarized scanning tunnelling microscopy images in FIG. 2c demonstrate the evolution of weakly pinned isolated skyrmions at low fields in FePd/Ir nanolayers[4,13,35]. The formation of lattices at the critical line $H_s(T)$ is impeded by the restricted mobility of pinned, isolated skyrmions, which in turn persist at their positions even in fields as low as H_{el}. Their interactions with neighbouring skyrmions and with the sample edges hamper the strip-out transition at H_{el}. Instead, there is an increase in the elliptical distortions, and skyrmions transform into a helical state[4]. The evolution of magnetic skyrmions in the presence of an applied field, and the role of disorder in their stability and dynamics, encouraged intensive efforts on the synthesis of composite materials and the design of devices for prospective applications[20,21,39,40,43–45]. The technological aspect of magnetic skyrmions has been duly addressed in recent reviews[21,45]. In this Perspective, we focus on the fundamental properties and address the stabilization mechanism within the general principles of soliton physics.

Magnetic skyrmions as solitons. The skyrmion energy E (see BOX 1) can be calculated with the ansatz

$$\theta(\rho) = 4\arctan[\exp(-\rho/R)], \quad (3)$$

where parameter R represents the skyrmion core radius. This trial function is based on the well-known Landau–Lifshitz solution for isolated domain walls[28] and provides a good fit to the solutions of Eq. 8. The skyrmion energy calculated with the ansatz above is reduced to the quadratic polynomial[4]

$$\mathcal{E}(R) = \mathcal{A} + \mathcal{B}R^2 - 3.02|D|R, \quad (4)$$

where $\mathcal{A} = 4.31\,A$; $\mathcal{B} = 1.59K + 1.39\mu_0 MH$, with D and A as defined in BOX 1. The minimization of $\mathcal{E}(R)$ yields the equilibrium skyrmion size

$$\overline{R}(H,K) = 1.51|D|/\mathcal{B}(H,K) \quad (5)$$

and the transition field $H_s(K)$. For cubic helimagnets, the model in Eq. 10 yields $H_s(0) = 0.760 H_D$ (compared with the rigorous value $0.801 H_D$ (FIG. 2c)).

The energy $\mathcal{E}(R)$ includes two competing contributions: the Dzyaloshinskii–Moriya energy (proportional to $-R$), which favours an unlimited extension of the skyrmion core ($R \to \infty$), and the energies of the uniaxial anisotropy, and the interaction with the applied magnetic field ($\mathcal{B} \propto R^2$), which tends to suppress the skyrmion ($R \to 0$). The equilibrium skyrmion size $\overline{R}$ in Eq. 5 forms because of a balance between these counteracting intrinsic forces. Similar competing processes (dispersion versus interaction with the seabed) underlie the formation of shallow water solitons (BOX 2). In both phenomena, the emerging localized states (solitons) correspond to the local minimum of the system and exhibit remarkable stability, which protects them against perturbations and preserves their shape. Notably, skyrmions demonstrate properties attributed to solitons and are described by methods of soliton physics (BOX 2) (for details, see REFS[2,4,32]).

Phase portraits of solutions. Further insight into the nature of magnetic skyrmions can be obtained by solving equation 8 in (BOX 1) with initial values $[\theta(0) = \pi, d\theta/d\rho(0) = -\eta]$. Any localized solution of this equation (shown in FIG. 2b) is among a set of parametrized profiles $\theta_{(\eta)}(\rho)$ $(0 < \eta < \infty)$ and corresponds to a fixed value of η. Typical profiles $\theta_{(\eta)}(\rho)$ (panel **f**) and the corresponding phase portraits ($\theta_{(\eta)}$, $d\theta_{(\eta)}/d\rho$) (panel **g**) are plotted in BOX 1. Most curves $\theta_{(\eta)}(\rho)$ oscillate around lines $\theta_{1,2} = \pm\pi/2$ (panel **f**). The corresponding curves in phase ($\theta_{(\eta)}$, $d\theta_{(\eta)}/d\rho$) spiral around attractor

points ($\pm\pi/2$, 0). In phase space ($\theta_{(\eta)}$, $d\theta_{(\eta)}/d\rho$), the presence of a singular curve is found among the manifold of spiralling curves, and it ends at saddle point (0,0) (panel **g**). This 'separatrix' line corresponds to the localized solution of Eq. 8.

As a matter of fact, localized solutions of Eq. 8 exist only for finite values of D. In centrosymmetric ferromagnets ($D=0$), the curves $\theta_{(\eta)}(\rho)$ ($0<\eta<\infty$) oscillate around the line $\theta_1=\pi/2$ whereas the corresponding phase portrait curves spiral around the attractor ($\pi/2$, 0). The geometrical images, which appear in the form of 'shooting trajectories', as well as the phase portraits of the solutions shown in BOX 1 demonstrate how Dzyaloshinskii–Moriya interactions can stabilize solutions for localized states. Thus, the basic properties of magnetic skyrmions can be elucidated without directly solving differential Eq. 2.

Skyrmion lattices

For a long time, the homochiral long-period structures emerging in magnetic materials with broken inversion symmetry were identified as one-dimensional modulations — helices[46]. Subsequently, it was established that in uniaxial non-centrosymmetric ferromagnets and in nanolayers of cubic helimagnets, the helical phases retain their thermodynamic stability in weak magnetic fields and transform into skyrmion lattices through a first-order transition at a critical field $H_1(T)$ (REFS[1–3,36]). At higher fields, the magnetic skyrmion lattices (FIG. 3a) correspond to the global minimum of the system[2,36]. Experimentally, the formation of a hexagonal skyrmion lattice is typically observed during the magnetic field-induced phase transition from the helical phase[8,15].

Solutions for skyrmion lattice cells describe a gradual localization of the skyrmion core and the expansion of the lattice period L with the increase of an applied magnetic field[2] (FIG. 3b). At $H_s(T)$, the skyrmion lattice transforms into the saturated state by an infinite expansion of the period ($L\rightarrow\infty$). Note that solutions for the skyrmion core have finite values at H_s. Hence, during transition into the saturated state, the skyrmion lattice transforms into an ensemble of isolated skyrmions. Theoretically, this transition is reversible, and, by decreasing the applied magnetic field (below H_s), the ensemble of isolated skyrmions should recondense to a skyrmion lattice. This, in fact, is one of the scenarios for the evolution of a skyrmion texture.

The transformation of a skyrmion lattice to the saturated state develops continuously, like a second-order phase transition[47]. According to Landau theory, second-order transitions occur between a lower-symmetry phase with a finite order parameter ϑ and a high-symmetry phase ($\vartheta=0$). During a phase transition, the order parameter decreases gradually and goes to zero at the critical point (that is, the lower-symmetry phase fades away). Take, for example, the order parameter of the ferromagnetic phase. In this case, the magnetization modulus $|\mathbf{M}|$ goes to zero at a distinct transition temperature (the Curie temperature), and the system turns into the paramagnetic phase.

However, a skyrmion lattice does not vanish at a critical field. Instead, it decomposes into isolated skyrmions. According to Pierre-Gilles De Gennes, phase transitions with a continuous decomposition of lower-symmetry phases belong to the nucleation type[48]. The continuous transition between helicoids and saturated phases proceeds in a similar way — namely, through sublimation and re-sublimation of homochiral isolated domain walls[10]. In fact, the magnetic-field-driven transitions of bubble domain lattices and stripe domains into a homogeneous phase belong to the nucleation type[28].

Kinsmen of magnetic skyrmions

From a mathematical perspective, solutions for multidimensional localized states arise only in field models containing either energy contributions linear with respect to spatial derivatives or with higher-order spatial derivatives[1,10,46]. The former are composed of Lifshitz invariants in Eq. 8 and describe, for example, Dzyaloshinskii–Moriya interactions in magnetic compounds with broken inversion symmetry[1,10,49]. In condensed matter, there are no physical interactions underlying energy contributions with higher-order spatial derivatives. However, Tony Skyrme introduced a stabilization term, quartic in the spatial derivatives (Skyrme mechanism), to describe low-energy dynamics of mesons and baryons[23,26]. Two-dimensional and three-dimensional localized solutions stabilized by the Skyrme mechanism are

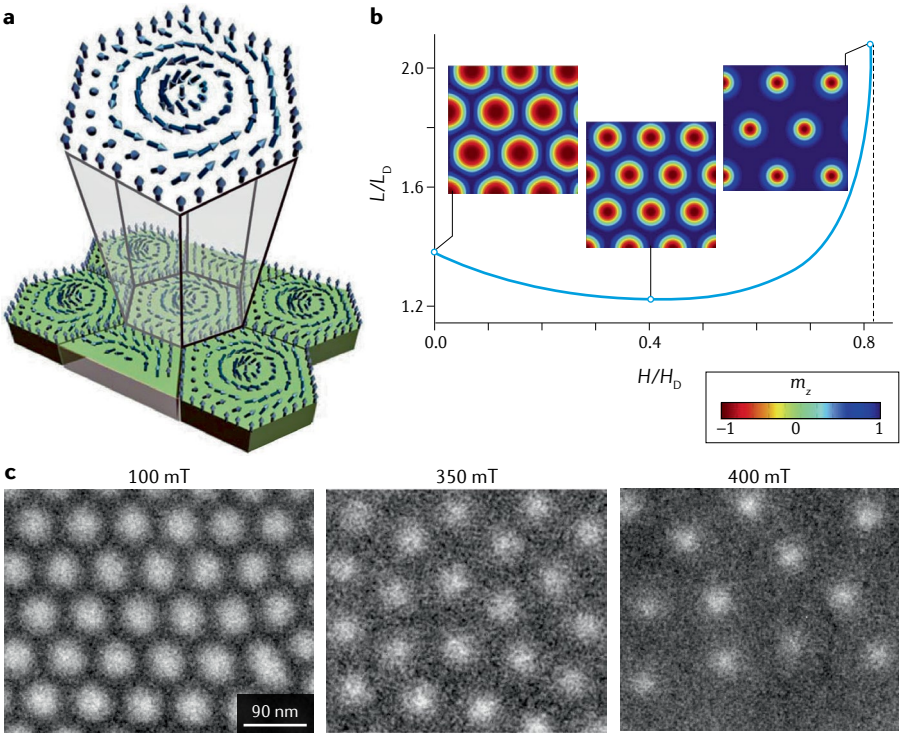

Fig. 3 | **Evolution of skyrmion lattices in an applied magnetic field. a** | Fragment of a hexagonal lattice with Bloch-type skyrmion cores. **b** | Equilibrium size of skyrmion cell L as a function of applied magnetic field H at zero anisotropy. L_D is the period of helical modulations at zero field and anisotropy, H_D is the saturation magnetic field. The insets show calculated contour plots $m_z(x,y)$ for $H/H_s=0$ (left inset), 0.5 (centre inset), 0.999 (right inset), where $H_s=0.801H_D$ is the the critical field of the phase transition (also marked by the dashed vertical line). **c** | Images of skyrmion textures in a thin layer of FeGe for different applied magnetic fields (100–400 mT) recorded by off-axis electron holography at $T=200$ K. The white scale bar indicates the L_D length. Panel **b** adapted from REF.[33], CC BY 3.0. Panel **c** adapted from REF.[34], CC BY 4.0.

intensively investigated with 'Faddeev–Skyrme' models[23,50]. The energy density functional is given by

$$w(\boldsymbol{v}) = a(\partial_i \boldsymbol{v})^2 + b(\partial_i \boldsymbol{v} \times \partial_j \boldsymbol{v})^2 + V(\boldsymbol{v}). \quad (6)$$

Here, the unity vector $\mathbf{v}$ is the order parameter, characteristic for the family of field models[50]. It consists of the common stiffness energy with constant a, the Skyrme energy with constant b, and the potential energy $V(v)$.

Non-centrosymmetric systems. In condensed-matter systems with broken inversion symmetry, such as ferroelectrics, chiral liquid crystals and multiferroics, interactions analogous to Dzyaloshinskii–Moriya coupling can provide the stabilization mechanism for multidimensional solitons. Indeed, cholesterics and other chiral nematics host various textures with chiral modulations[49]. Among them, two-dimensional axisymmetric localized strings, analogous to magnetic skyrmions, have been observed in thin layers with strong perpendicular surface pinning (homeotropic anchoring)[51,52]. Furthermore, axisymmetric skyrmions have been observed in layered oxides with spontaneous electric polarization (ferroelectrics)[53].

Skyrmion–bubble hybrids. Localized magnetic patterns in nanolayers and multilayer magnetic architectures, emerge under the combined influence of surface/interface-induced Dzyaloshinskii–Moriya interactions and magneto-dipolar coupling. These localized states may be considered 'skyrmion–bubble hybrids', exhibiting magnetic properties attributed to chiral skyrmions and magnetic domains. They are distinct from the classical cylindrical domains (bubbles) observed in thin films with strong perpendicular magnetic anisotropy. Magnetic bubbles are areas of antiparallel magnetization, separated from the magnetically saturated matrix by thin domain walls[28]. Importantly, although magnetic bubbles and skyrmions have the same topology, they are fundamentally different physical objects. Bubbles are intrinsically unstable magnetic domains, which can be stabilized by surface demagnetization effects in confined magnets and depend on the shape of a magnetized body[28].

Skyrmion–bubble hybrids are a new class of chiral localized states. The modulation of the geometry or composition of a magnetic multilayer promises fine control over the frequency response associated with skyrmions and the corresponding gyration of the topological charge, which is dependent on the interlayer dipolar coupling within the heterostructure. For example, raising this coupling may increase the skyrmion radius and tune the frequency and field response of its resonance. This intrinsic adjustability highlights one of the potential advantages of chiral magnetic multilayers.

Exchange modulations. These modulated textures emerge in an extended group of centrosymmetric magnetic compounds and are stabilized by competing non-local exchange interactions[46]. Unlike homochiral and long-periodic modulations induced by Dzyaloshinskii–Moriya interactions, exchange modulations are characterized by periods of a few lattice constants and arbitrary rotation sense. These give rise to numerous short-period spirals in rare earth metals and related materials[46]. There has been evidence for nanoscale magnetic heterostructures exhibiting multidimensional short-period modulated states supported by complex non-local exchange interactions[12]. Instead of continuum (field) models, such short-period modulations are described either within discrete models[4,29,37,54] or by applying methods of quantum magnetism[12,55]. The fundamental properties of magnetic skyrmions (including stability criteria) have been derived within field models and do not apply to properties of short-period modulations (independent of the stabilization mechanism). Thus, the multidimensional short-period modulated states derived in REFS[12,29,37,54] should not be confused with magnetic skyrmions and other solitons. In a continuum limit, discrete models for exchange modulations reduce to energy functionals of the type in Eq. 5 (REFS[46,56,57]) and establish relations between exchange modulations and field models, with the Skyrme stabilization mechanism.

Outlook

This Perspective addresses the physical foundations of magnetic skyrmions and aims to serve as an intelligible guide to the essential principles governing the properties of magnetic skyrmions in condensed-matter physics. Understanding the formation and evolution of these solitonic states within a conceptual framework helps to bring theoretical findings to the lab. Specifically, the underlying crystallographic structure of chiral magnets with broken inversion symmetry induces competing magnetic interactions, with the emerging localized states exhibiting remarkable stability, protecting them against perturbations and preserving their shape. In practice, the basic physical properties illustrate that these spin textures can be created and manipulated using readily available tools in a variety of bulk crystals and synthetic architectures.

Box 2 | Shallow water solitons

Mathematically, shallow water waves propagating along the x-axis are described by the one nonlinear equation:

$$\frac{1}{v_0}\frac{\partial \eta}{\partial t} + \frac{\partial \eta}{\partial x} + \underbrace{\frac{h^2}{6}\frac{\partial^3 \eta}{\partial x^3}}_{\text{dispersion}} + \underbrace{\frac{3}{2h}\eta\frac{\partial \eta}{\partial x}}_{\text{interaction with seabed}} = 0, \quad (11)$$

known as the Korteweg–de Vries (KdV) equation. Here, the water surface elevation $\eta(x,t)$ depends on x and time t; h is the water depth and g is gravitational acceleration. The first two terms in the KdV equation yield solutions for non-dispersive waves propagating with speed $v_0 = \sqrt{gh}$; the next two terms describe the competing contributions of dispersion ($\propto h^2$) and the interaction with the seabed ($\propto 1/h$).

In extremely shallow water (that is, when h is a factor of 20 or more smaller than the wavelength L), the last term suppresses dispersion processes and stabilizes solutions for solitary waves with bell-shaped profiles (solitons)[22]

$$\eta_s(x,t) = \frac{2\gamma^2}{\cosh^2[\gamma(x - 4\gamma^2 t - x_0)]}, \quad (12)$$

where γ is a material parameter including the speed, width and height of the wave. The calculated wave profiles $\eta_s(x, t)$ plotted for different values of parameter γ in the figure are in good agreement with laboratory reconstructions of Russell's soliton in a shallow water channel[24] (see video in Related link).

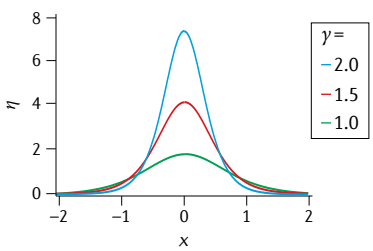

Alexei N. Bogdanov[1,2] and Christos Panagopoulos[3]

[1]IFW Dresden, Dresden, Germany.

[2]Chirality Research Center, Hiroshima University, Hiroshima, Japan.

[3]Division of Physics and Applied Physics, School of Physical and Mathematical Sciences, Nanyang Technological University, Singapore, Singapore.

e-mail: christos@ntu.edu.sg

https://doi.org/10.1038/s42254-020-0203-7

Published online 29 July 2020

1. Bogdanov, A. N. & Yablonskii, D. A. Thermodynamically stable 'vortices' in magnetically ordered crystals. The mixed state of magnets. *Sov. Phys. JETP* **68**, 101–103 (1989).
2. Bogdanov, A. & Hubert, A. Thermodynamically stable magnetic vortex states in magnetic crystals. *J. Magn. Magn. Mater.* **138**, 255–269 (1994).
3. Rößler, U. K., Bogdanov, A. N. & Pfleiderer, C. Spontaneous skyrmion ground states in magnetic metals. *Nature* **442**, 797–801 (2006).
4. Leonov, A. O. et al. The properties of isolated chiral skyrmions in thin magnetic films. *N. J. Phys.* **18**, 065003 (2016).
5. Mühlbauer, S. et al. Skyrmion lattice in a chiral magnet. *Science* **323**, 915–919 (2009).
6. Pappas, C. et al. Chiral paramagnetic skyrmion-like phase in MnSi. *Phys. Rev. Lett.* **102**, 197202 (2009).
7. Yu, X. Z. et al. Real-space observation of a two-dimensional skyrmion crystal. *Nature* **465**, 901–903 (2010).
8. Yu, X. Z. et al. Near room-temperature formation of a skyrmion crystal in thin-films of the helimagnet FeGe. *Nat. Mater.* **10**, 106–109 (2011).
9. Derrick, G. H. Comments on nonlinear wave equations as models for elementary particles. *J. Math. Phys.* **5**, 1252–1254 (1964).
10. Dzyaloshinskii, I. E. Theory of helicoidal structures in antiferromagnets. *Sov. Phys. JETP* **19**, 960–971 (1964).
11. Bogdanov, A. & Hubert, A. The properties of isolated magnetic vortices. *Phys. Stat. Sol.* **186**, 527 (1994).
12. Heinze, S. et al. Spontaneous atomic-scale magnetic skyrmion lattice in two dimensions. *Nat. Phys.* **7**, 713–718 (2011).
13. Romming, N. et al. Writing and deleting single magnetic skyrmions. *Science* **341**, 636–639 (2013).
14. Langner, M. C. et al. Coupled skyrmion sublattices in Cu_2OSeO_3. *Phys. Rev. Lett.* **112**, 167202 (2014).
15. Kézsmárki, I. et al. Néel-type skyrmion lattice with confined orientation in the polar magnetic semiconductor GaV_4S_8. *Nat. Mater.* **14**, 1116–1122 (2015).
16. Zhang, S. L. et al. Multidomain skyrmion lattice state in Cu_2OSeO_3. *Nano Lett.* **16**, 3285–3291 (2016).
17. Fujishiro, Y. et al. Topological transitions among skyrmion- and hedgehog-lattice states in cubic chiral magnets. *Nat. Commun.* **10**, 1059 (2019).
18. Zefang, D. et al. Observation of magnetic skyrmion bubbles in a van der Waals ferromagnet Fe_3GeTe_2. *Nano Lett.* **20**, 868–873 (2020).
19. Nayak, A. K. et al. Magnetic antiskyrmions above room temperature in tetragonal Heusler materials. *Nature* **548**, 561–566 (2017).
20. Fert, A., Cros, V. & Sampaio, J. Skyrmions on the track. *Nat. Nanotechnol.* **8**, 152–156 (2013).
21. Fert, A., Reyren, N. & Cros, V. Magnetic skyrmions: advances in physics and potential applications. *Nat. Rev. Mater.* **2**, 17031 (2017).
22. Remoissenet, M. *Waves Called Solitons. Concepts and Experiments*, 328 (Springer, 2003).
23. Manton, N. & Sutcliffe, P. *Topological Solitons* (Cambridge Univ. Press, 2004).
24. Bogdanov, A. N. & Panagopoulos, C. The emergence of magnetic skyrmions. *Phys. Today* **73**, 44–49 (2020).
25. Zabusky, N. J. & Kruskal, M. D. Interaction of solitons in a collisionless plasma and the recurrence of initial states. *Phys. Rev. Lett.* **15**, 240–243 (1965).
26. Skyrme, T. H. A non-linear field theory. *Proc. R. Soc. A* **260**, 127–138 (1961).
27. Brown, G. E. & Rho, M. (eds) *The Multifaceted Skyrmion* (World Scientific, 2010).
28. Hubert, A. & Schäfer, R. *Magnetic Domains* (Springer, 1998).
29. Okubo, T., Chung, S. & Kawamura, H. Multiple-q states and the skyrmion lattice of the triangular-lattice Heisenberg antiferromagnet under magnetic fields. *Phys. Rev. Lett.* **108**, 017206 (2012).
30. White R. M. *Quantum Theory of Magnetism*, 362 (Springer, 2007).
31. Bak, P. & Jensen, M. H. Theory of helical magnetic structures and phase transitions in MnSi and FeGe. *J. Phys. C* **13**, L881–L885 (1980).
32. Bogdanov, A. & Hubert, A. The stability of vortex-like structures in uniaxial ferromagnets. *J. Magn. Magn. Mater.* **195**, 182–192 (1999).
33. Leonov, A. O. & Bogdanov, A. N. Crossover of skyrmion and helical modulations in noncentrosymmetric ferromagnets. *N. J. Phys.* **20**, 043017 (2018).
34. Kovács, A. et al. Mapping the magnetization fine structure of a lattice of Bloch-type skyrmions in an FeGe thin film. *Appl. Phys. Lett.* **111**, 192410 (2017).
35. Romming, N., Kubetzka, A., Hanneken, C., Bergmann, K. V. & Wiesendanger, R. Field-dependent size and shape of single magnetic skyrmions. *Phys. Rev. Lett.* **114**, 177203 (2015).
36. Wilson, M. N., Butenko, A. B., Bogdanov, A. N. & Monchesky, T. L. Chiral skyrmions in cubic helimagnet films: the role of uniaxial anisotropy. *Phys. Rev. B* **89**, 094411 (2014).
37. Siemens, A., Zhang, Y., Hagemeister, J., Vedmedenko, E. Y. & Wiesendanger, R. Minimal radius of magnetic skyrmions: statics and dynamics. *N. J. Phys.* **18**, 045021 (2016).
38. Leonov, A. O. et al. Chiral surface twists and skyrmion stability in nanolayers of cubic helimagnets. *Phys. Rev. Lett.* **117**, 087202 (2016).
39. Moreau-Luchaire, C. et al. Additive interfacial chiral interaction in multilayers for stabilization of small individual skyrmions at room temperature. *Nat. Nanotechnol.* **11**, 444–448 (2016).
40. Duong, N. K. et al. Stabilizing zero-field skyrmions in Ir/Fe/Co/Pt thin film multilayers by magnetic history control. *Appl. Phys. Lett.* **114**, 072401 (2019).
41. McGrouther, D. et al. Internal structure of hexagonal skyrmion lattices in cubic helimagnets. *N. J. Phys.* **18**, 095004 (2016).
42. Yu, X. Z. et al. Variation of skyrmion forms and their stability in MnSi thin plates. *Phys. Rev. B* **91**, 054411 (2015).
43. Soumyanarayanan, A., Reyren, N., Fert, A. & Panagopoulos, C. Emergent phenomena induced by spin–orbit coupling at surfaces and interfaces. *Nature* **539**, 509–517 (2016).
44. Woo, S. et al. Observation of room temperature magnetic skyrmions and their current-driven dynamics in ultrathin Co films. *Nat. Mater.* **15**, 501–506 (2016).
45. Wiesendanger, R. Nanoscale magnetic skyrmions in metallic films and multilayers: a new twist for spintronics. *Nat. Rev. Mater.* **1**, 16044 (2016).
46. Izyumov, Yu. A. Modulated, or long-periodic, magnetic structures of crystals. *Sov. Phys. Usp.* **27**, 845–867 (1984).
47. Landau, L. D. & Lifshitz, E. M. *Statistical Physics* 3rd edition, Part 1 (Pergamon, 1980).
48. De Gennes P. G. *Fluctuations, Instabilities, and Phase Transitions* (ed. Riste, T.) (Plenum, 1975).
49. Wright, D. C. & Mermin, N. D. Crystalline liquids: the blue phases. *Rev. Mod. Phys.* **61**, 385–432 (1989).
50. Faddeev, L. D. Some comments on the many-dimensional solitons. *Lett. Math. Phys.* **1**, 289–293 (1976).
51. Leonov, A. O., Dragunov, I. E., U. K. Rößler, U. K. & Bogdanov, A. N. Theory of skyrmion states in liquid crystals. *Phys. Rev. E* **90**, 042502 (2014).
52. Ackerman, P. J. et al. Two-dimensional skyrmions and other solitonic structures in confinement-frustrated chiral nematics. *Phys. Rev. E* **90**, 012505 (2014).
53. Das, S. et al. Observation of room-temperature polar skyrmions. *Nature* **568**, 368–372 (2019).
54. Leonov, A. O. & Mostovoy, M. Multiply periodic states and isolated skyrmions in an anisotropic frustrated magnet. *Nat. Commun.* **6**, 8275 (2015).
55. Romming, N. et al. Competition of Dzyaloshinskii–Moriya and higher-order exchange interactions in Rh/Fe atomic bilayers on Ir (111). *Phys. Rev. Lett.* **120**, 207201 (2018).
56. Hubert, A. *Theorie der Domänenwände in geordneten Medien* (Springer, 1974).
57. Melnichuk, P. I., Bogdanov, A. N., Rößler, U. K. & Müller, K.-H. Hubert model for modulated states in systems with competing exchange interactions. *J. Magn. Magn. Mater.* **248**, 142–150 (2002).

Acknowledgements
The authors acknowledge A. Fert and R. Wiesendanger for discussions. A.N.B. thanks M. Ochi and K. Inoue for hospitality and collaboration during his stay at Hiroshima University. This work was supported in Germany by the Deutscher Forschungsgemeinschaft through SPP2137 'Skyrmionics', and in Singapore by the Ministry of Education (MOE), under its MOE AcRF Tier 3 Award MOE2018-T3-1-002, and the National Research Foundation (NRF) Singapore under NRF Investigatorship (no. NRF-NRFI2015-04).

Author contributions
Both authors have read, discussed and contributed to the writing of the manuscript.

Competing interests
The authors declare no competing interests.

Peer review information
Nature Reviews Physics thanks the anonymous reviewers for their contribution to the peer review of this work.

Publisher's note
Springer Nature remains neutral with regard to jurisdictional claims in published maps and institutional affiliations.

RELATED LINKS
Pizzo, N. Shallow water wave generation: www.youtube.com/watch?v=w-oDnvbV8mY